European Journal of Pharmacology 887 (2020) 173525

Contents lists available at ScienceDirect

European Journal of Pharmacology

journal homepage: www.elsevier.com/locate/ejphar

Full length article

Inhibition of intracellular Ca^{2+} mobilization and potassium channels activation are involved in the vasorelaxation induced by 7-hydroxycoumarin

Quiara Lovatti Alves [a,b], Raiana dos Anjos Moraes [a,b], Thamires Quadros Froes [c], Marcelo Santos Castilho [c], Rodrigo Santos Aquino de Araújo [d], José Maria Barbosa-Filho [d], Cássio Santana Meira [b], Milena Botelho Pereira Soares [b], Darízy Flávia Silva [a,b,*]

[a] Laboratory of Cardiovascular Physiology and Pharmacology, Federal University of Bahia, Salvador, BA, 40110-902, Brazil
[b] Gonçalo Moniz Institute, Oswaldo Cruz Foundation, FIOCRUZ, Bahia, Brazil
[c] Laboratory of Bioinformatics and Molecular Modeling, Faculty of Pharmacy, Federal University of Bahia, Salvador, BA, 40170-115, Brazil
[d] Laboratory of Pharmaceutical Technology, Department of Physiology and Pathology, Federal University of Paraíba, João Pessoa, PB, 58051-970, Brazil

ARTICLE INFO

Keywords:
7-Hydroxycoumarin
Vasorelaxation
K^+ channels
FTMap
Docking

ABSTRACT

Coumarins exhibit a wide variety of biological effects, including activities in the cardiovascular system and the aim of this study was to evaluate the vascular therapeutic potential of 7-Hydroxicoumarin (7-HC). The vascular effects induced by 7-HC (0.001 μM–300 μM), were investigated by *in vitro* approaches using isometric tension measurements in rat superior mesenteric arteries and by *in silico* assays using Ligand-based analysis. Our results suggest that the vasorelaxant effect of 7-HC seems to rely on potassium channels, notably through large conductance Ca^{2+}-activated K^+ (BK_{Ca}) channels activation. In fact, 7-HC (300 μM) significantly reduced $CaCl_2$-induced contraction as well as the reduction of intracellular calcium mobilization. However, the relaxation induced by 7-HC was independent of store-operated calcium entry (SOCE). Moreover, *in silico* analysis suggests that potassium channels have a common binding pocket, where 7-HC may bind and hint that its binding profile is more similar to quinine's than verapamil's. These results are compatible with the inhibition of Ca^{2+} release from intracellular stores, which is prompted by phenylephrine and caffeine. Taken together, these results demonstrate a therapeutic potential of 7-HC on the cardiovascular system, making it a promising lead compound for the development of drugs useful in the treatment of cardiovascular diseases.

1. Introduction

Cardiovascular diseases are and will continue to be among the major health problems of today's society (World Health Organization et al., 2013), and hypertension is one of the strongest risk factors for most cardiovascular diseases (Kjeldsen, 2018). In the last few decades, many medicinal plants and their constituents have had their hypotensive and antihypertensive therapeutic value validated (Tabassum and Ahmad, 2011).

The use of medicinal plants for the treatment, cure and prevention of diseases is as old as humanity itself (Petrovska, 2012) and according to fossil records, the human use of plants as medicines goes back 60,000 years (Solecki, 1975). Natural products from medicinal plants have proved to be an abundant source of biologically active compounds, many of which have been the basis for the development of new chemical entities for the pharmaceutical industry (Hotwani et al., 2014). More than 3400 coumarins have already been identified from natural sources (Markham and Dog, 2013) and many studies have demonstrated that 7-Hydroxycoumarin (7-HC) (Fig. 1) presents pharmacological effects of interest, such as antifungal, antinociceptive and anti-inflammatory properties (De Almeida Barros et al., 2010; de Araújo et al., 2013; De Lima et al., 2011). Several coumarins have known vasorelaxant activities (He et al., 2007; Lemmich et al., 1983; Oliveira et al., 2001) and 7-HC was described as promoting increased coronary blood flow and caused positive inotropism in the rat heart, as well as a direct vasorelaxant effect on coronary arteries (Baccard et al., 2000). Furthermore,

* Corresponding author. Laboratory of Cardiovascular Physiology and Pharmacology, Federal University of Bahia, Avenida, Reitor Miguel Calmon, Vale do Canela, 40110-902, Salvador, Bahia, Brazil.
E-mail address: darizy@gmail.com (D.F. Silva).

https://doi.org/10.1016/j.ejphar.2020.173525
Received 19 May 2020; Received in revised form 24 August 2020; Accepted 28 August 2020
Available online 1 September 2020

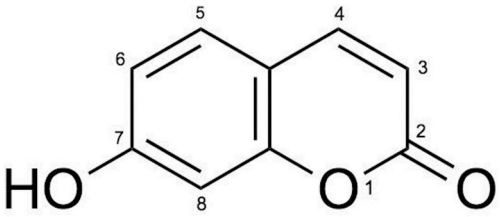

Fig. 1. Chemical structure of 7-Hydroxycoumarin.

7-HC protects isoproterenol-induced myocardial infarction in rats through free radical scavenging (Jagadeesh et al., 2016). Despite its vasorelaxant and cardiac potential, there are no studies exploring 7-HC's effects and mechanisms of action.

The major aim of this work is to evaluate the vascular effects of 7-HC and specifically to describe the mechanisms of action involved in the observed responses.

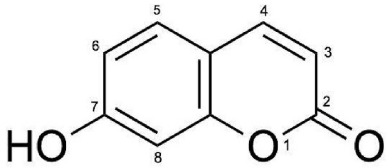

2. Material and methods

2.1. Plant material and extraction and isolation of 7-HC

The aerial parts (2000 g) of Typha domingensis Pers. Were collected for first in March 2002 in Bravo, State of Bahia and after in December 2005 near the city of Santa Rita, State of Paraíba, Brazil. The aerial parts of this plant were extracted with 95% ethanol at room temperature, as described by Vasconcelos and colleagues (Vasconcelos et al., 2009), and the isolated compounds were identified as coumarin based on 1H NMR, 13C NMR, COSY, HMQC and HMBC spectroscopic data and compared with those reported in the literature. 7-HC was kindly provided by Dr. José Maria Barbosa from the Pharmaceutical Technology Laboratory of the Federal University of Paraíba.

2.2. Animals

Male Wistar rats weighing 250–350 g, were obtained from the Neurosciences Laboratory of the Health Sciences Institute at the Federal University of Bahia (ICS/UFBA). Animals were housed under controlled temperature (21 ± 1 °C) and day/night cycles (6:00–18:00 h), with free access to food and water. The tests were performed in accordance with the guidelines of care and use of laboratory rats, adopted by the National Council for Animal Experiments Control (CONCEA - BRAZIL) and were approved for use by the Ethics Committee on Animal Use from the Institute of Health Sciences, Federal University of Bahia (CEUA-ICS protocol/UFBA nº. 130/2017).

2.3. Drugs and solutions

The drugs used in this study were: L-phenylephrine hydrochloride, acetylcholine chloride, barium chloride ($BaCl_2$), 4-aminopyridine (4-AP), tetraethylammonium (TEA), iberiotoxin (IbTx), glibenclamide (Glib), caffeine and cremophor, all acquired from Sigma-Aldrich (Sigma Chemical Co., Saint Louis, MO, USA). All drugs were dissolved in distilled water. K^+-depolarizing solutions (KCl 20 and 60 mM) were prepared by replacing equimolar NaCl by 20 or 60 mM of KCl.

For the preparation of the 7-hydroxycoumarin solutions, 7-HC was solubilized in cremophor and diluted to the desired concentrations with distilled water (*in vitro* assay). The final concentration of cremophor in the organ bath never exceeded 0.003% and had no effect when tested in control preparations. Tyrode's physiological solution was used throughout all arterial experiments with the following compositions (mM): NaCl, 158.3; KCl, 4.0; $CaCl_2$, 2.0; $MgCl_2$, 1.05; NaH_2PO_4, 0.42; $NaHCO_3$, 10.0, and glucose, 5.6, at 37 °C were acquired from either Sigma (Sigma-Aldrich, St. Louis, USA) or Vetec (Rio de Janeiro, Brazil).

2.4. In vitro assays

2.4.1. Cytotoxicity in mammalian cells

H9c2 heart myoblast cell line were plated onto 96-well plates at a cell density of 5×10^3 cells/well in Dulbecco's modified Eagle medium (DMEM; Life Technologies, GIBCO-BRL, Gaithersburg, MD, USA) supplemented with 10% fetal bovine serum (FBS; GIBCO), and 50 μg/ml of gentamycin (Novafarma, Anápolis, GO, Brazil) and incubated for 24 h at 37 °C and 5% CO_2. Following this, each sample was added at five concentrations of 7-HC (25, 50 and 100 μM) in triplicate and incubated for 72 h. Twenty μl/well of AlamarBlue (Invitrogen, Carlsbad, CA) were added to the plates during 10 h. Colorimetric readings were performed at 570 and 600 nm. Concentration that reduced cell viability by 50% (CC_{50}) were calculated using data-points gathered from three independent experiments. Gentian violet was used as positive control.

2.4.2. Isolation of superior mesenteric arteries

Wistar normotensive rats were euthanized in a CO_2 chamber, and the middle portion of superior mesenteric arteries were removed (Silva et al., 2011) and cleaned of connective tissue and fat. Mesenteric rings (2 mm) were placed in an organ bath with physiological Tyrode's, maintained at 37°C and pH 7.4 and gassed with a carbogenic mixture (95% O_2 and 5% CO_2). Rings were stabilized with an optimal resting tension of 0.75 g for 60 min. The isometric tension was recorded by a force transducer (Insight, Ribeirão Preto, SP, Brazil) coupled to an amplifier-recorder (Insight, Ribeirão Preto, SP, Brazil) and to a personal computer equipped with a data acquisition software. The presence of functional endothelium was assessed by the ability of acetylcholine (1 μM) to induce at least a 90% relaxation response in phenylephrine (Phe, 1 μM) pre-contracted mesenteric artery rings. Rings that relaxed less than 10% were considered endothelium-denuded/damaged.

2.4.3. Effect of 7-HC on the vasculature

After the stabilization period, two successive contractions of similar magnitude were induced with phenylephrine 1 μM (Phe), an alpha1-adrenergic agonist, in endothelium-intact and -denuded rings. In the tonic phase of the second contraction, increasing concentrations of 7-HC (0.001 μM–300 μM) were cumulatively added to the organ bath and the effects were compared. The vasorelaxant effects of 7-HC were also assessed following a 60 mM KCl -induced contraction in endothelium-denuded arteries. Additionally, 7-HC was added to endothelium-intact vessels at basal tone in order to examine the effect of 7-HC on spontaneous muscle tone. To examine the ability of the mesenteric artery to contract after exposure to 7-HC, preparations were washed three times after 7-HC addition and a second contraction with 60 mM KCl was obtained.

2.4.4. Evaluation of K^+ channel activity in the 7-HC-induced vasorelaxation response

To investigate the mechanism involved in 7-HC induced relaxation, endothelium-denuded ring preparations were pre-incubated with phenylephrine in Tyrode's solution with high K^+ concentration (20 mM) and the relaxation effect induced by 7-HC (0.001 μM–300 μM) was observed.

In another set of experiments, the involvement of K^+ channels in the vasorelaxant response induced by 7-HC was evaluated following pre-incubation of the endothelium-denuded rings for 30 min with different pharmacological agents: TEA (1 mM), a non-selective blocker of large conductance Ca^{2+}-activated K^+ (BK_{Ca}) channels (Langton et al., 1991),

iberiotoxin (50 nM), a selective blocker of BK_{Ca} channel (Frieden et al., 1999); 4-AP (1 mM), a voltage-operated K^+ channel (K_V) blocker (Wang et al., 2008) and $BaCl_2$ (30 μM), a blocker of inward rectifying K^+ channels (K_{ir}) (Kawabata et al., 2004), glibenclamide (10 μM), a specific ATP-sensitive K^+ (K_{ATP}) channel subtype selective blocker (Insuk et al., 2003).

2.4.5. Investigation of the effects induced by 7-HC on Ca^{2+} influx

To investigate the effects of 7-HC on Ca^{2+} influx in endothelium-denuded rings, cumulative concentrations of $CaCl_2$ (100 μM–10,000 μM) were added to a depolarization medium of Ca^{2+}-free Tyrode's solution (60 mM KCl) during 15 min, in the absence (control) or presence of 7-HC concentrations (1; 10 and 100 μM). In another set of experiments, to investigate Ca^{2+} influx through SOCE (store-operated calcium entry), we performed experiments using SKF-96365 (10 μM), a non-specific inhibitor of SOC (Chen et al., 2013). Endothelium-denuded rings were pre-incubated with SKF-96365 (10 μM) for 30 min and subsequently Phe was added.

2.4.6. Investigation of 7-HC-induced mobilization of calcium from intracellular stores

After the stabilization period, vessels were pre-contracted with 60 mM KCl for 3 min, then washed with a Ca^{2+}-free tyrode solution containing EGTA 1 mM, followed by the addition of 1 μM phenylephrine (organ bath at 37 °C) or 20 mM caffeine (organ bath at 23 °C). Rings were rinsed with tyrode's physiological solution, and 60 mM KCl was added for 3 min to load the Ca^{2+} stores within the vascular smooth muscle. This procedure was repeated until two transient contractions of similar magnitude were obtained. Next, this experimental protocol was repeated by incubating 7-HC at different concentrations (30 and 300 μM) in Ca^{2+}-free tyrode solution for 5 min, which was followed by application of phenylephrine or caffeine, as previously described (Sakata and Karaki, 1991). The role of 7-HC on the mobilization of calcium from intracellular stores was assessed by comparing phenylephrine or caffeine mediated contraction in the absence and presence of 7-HC via IP_3 receptors and ryanodine receptors, respectively.

2.5. In silico assays

2.5.1. Comparison of druggable and borderline pockets in potassium channels

The 3D coordinates from BK_{Ca} (3NAF, 6V3G, 6V22, 6V35, 6V38), K_{ATP} (5YKE, 5YW7, 5 YWD, 6C3O, 6JB3, 6PZ9, 6PZA, 6PZB, 6PZC, 6PZI), K_{ir} (1U4F, 2GIX) and K_v (3LUT, 6 EBL, 6 EBM, 1QDW, 1QDV, 1DSX, 2A79) available in PDB databank (www.rcsb.org) had their putative binding sites predicted with FTMap server (https://ftmap.bu.edu/login.php). Briefly, FTMap samples the protein surface with 16 small molecule probes in order to find regions (consensus clusters-CS) that have a high probability to bind the probes. The CSs are ranked according to their number of probes and those CSs with five or less probes are discarded. Next, all the combinations of up to 3 CSs are calculated and their center-to-center distance (CD), and maximum dimension (MD) measured. Ensembles that follow the rules described by Kozakov and coworkers (Kozakov et al., 2015) and whose first CS (CS0) > 16 probes were classified as "druggable". In case the CS0 has between 13 and 16 probes, the ensembles were considered as "borderline". All the analysis were carried out with the potassium channels in the monomeric and oligomeric forms.

The residues within 4 Å of either a druggable or a borderline ensemble of CSs were employed to carry out a pocket similarity comparison, as available in pocket match server (http://proline.physics.iisc.ernet.in/pocketmatch/). Briefly, a set of 90 geometrical and chemical descriptor are calculated for each binding site and then pairwise compared (Yeturu and Chandra, 2008). The binding sites were compared according to their Pmin-score, since the size of the binding-sites are dissimilar. Only binding sites with P-min score >0.60 to two different potassium channels were considered for docking studies.

2.5.2. Pocket similarity analysis and docking studies

The 3D coordinates from potassium channels with resolution >3.5 Å were discarded. The remaining structures (BK_{Ca} (PDB ID 3NAF), 6PZA K_{ATP} (PDB ID 6PZA), K_{ir} (PDB ID 1U4F), and K_V (PDB ID: 3LUT)) were added hydrogen atoms in H-bonding orientation, and, subsequently, "Kollman all" charges, as available in "prepare structure biopolymer" module from Sybyl-X 2.1. Next, the search space (protomol) was defined using the binding sites selected previously, and default Threshold (0.5) and bloat (0.0) parameters, as available in SURFLEX-DOCK(Jain, 2007). The ligand (7-HC) was prepared as described in "ligand similarity analysis" section. The three best ranked poses, according to SURFLEX-DOCK scoring function, were visually analyzed within Pymol and then depicted in a 2D diagram, built with LigPlus software (RA and MB, 2011).

2.5.3. Ligand similarity analysis

The chemical similarity among 7-HC and 6 BK_{Ca} blockers were calculated using default parameters from the SURFLEX-SIM software, available in SYBYL-X 2.0 platform. Briefly, the 2D structures of all molecules were drawn on ChemBioDraw v16. software (Cambridge software ®), converted to 3D format and then energy minimized with Tripos force field (convergence criteria 0.01 kcal/mol and dielectric constant = 80). Then, 7-HC was employed as a template, upon which BK_{Ca} blockers (Paxiline, Verapamil, ketamine, Tetrandrine, Quinine, Clotrimazole) (Yu et al., 2016) were flexibly superposed, according to their morphological similarity, which compares the molecules based on their putative interaction profile within a hypothetical binding site. In order to reduce the root mean square deviation (rmsd) among molecules, pre-run and post-run minimization options were employed. Similarity scores range from 0.0 to 10.0, with higher values indicating higher 3D similarity (Yera et al., 2011).

2.6. Data analysis

The values were expressed as mean ± S.E.M. and "n" represents a number of mesenteric artery rings obtained from different rats. Statistical significance was determined by Student's t-test or One-way ANOVA followed by Bonferroni's post-test, when appropriate. Values of $P < 0.05$ were considered statistically significant. All statistical calculations were performed with Prism software version 5.0 (GraphPad Software Inc. La Jolla, CA, USA).

3. Results

3.1. Lack of cytotoxicity in H9c2 heart myoblast cell line treated by 7-HC

Fig. 2 shows that addition of 7-HC, at concentrations of 25, 50 and 100 μM, did not result in alterations of H9c2 cell proliferation. Gentian violet (GV) was used as positive control and caused a significant loss of cell viability (Fig. 2).

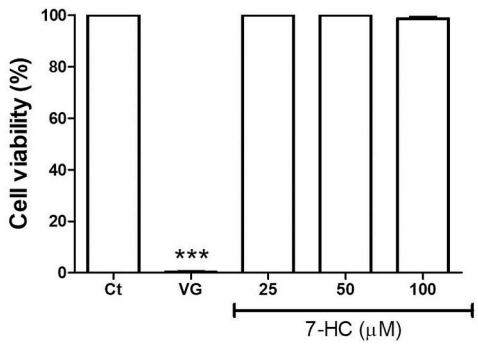

Fig. 2. Absence of cytotoxic effect of 7-HC on H9c2 cells. Ct: Control, VG: Gentian violet. ***P<0.001 vs control.

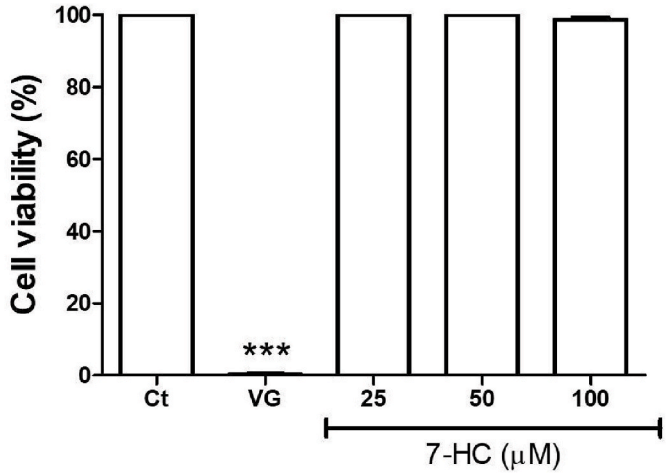

3.2. 7-HC induce endothelium-independent-relaxation in mesenteric artery

As shown in Fig. 3A, 7-HC (0.001 μM–300 μM) induced concentration-dependent relaxation in pre-contracted (Phe, 1 μM) mesenteric artery rings with or without endothelium [Effect [300 μM] = 94.9 ± 6.8%, (n = 5); Effect [300 μM] = 96.2 ± 7.1%, (n = 7), respectively]. This response was significantly different when compared to rings contracted with KCl 60 mM, Effect [300 μM] = 60.3 ± 7,4%, (n = 5) (**P < 0.01) (Fig. 3B). To assess tissue viability after the concentration response curves to 7-HC (0.001 μM–300 μM), a subsequent KCl-induced contraction (60 mM) was performed. There was no significant difference in the contractile ability of vascular rings before or after administration of cumulative concentrations of 7-HC, indicating that the 7-HC (at least the concentrations investigated) did not induce toxic effects or directly interfere with the arterial contractile machinery. Furthermore, there was no significant change in basal tone following administration of 7-HC (data not shown).

3.3. Vasorelaxation induced by 7-HC involves K^+ channels activation

To evaluate the participation of K^+ channels during 7-HC-mediated vasorelaxation response, experiments were performed using endothelium denuded vascular rings and contracted with Phe (1 μM) in the presence of a Tyrode solution containing 20 mM KCl. The partial blocking of K^+ efflux by elevating the extracellular K^+ concentration ($[K^+]e$) to 20 mM resulted in a significant reduction of the vasorelaxant effect following cumulative administration of 7-HC (0.001 μM–300 μM) with significant changes in the values of [300 μM] [72.1 ± 8, (n = 7) (*P < 0.05)] (Fig. 4A/4C/4D). Interestingly, the 7-HC-induced vasorelaxation was attenuated in the presence of TEA (1 mM) (Fig. 4 B/4 E) and Iberiotoxin (IbTx 50 nM) (Fig. 4 B/4 F) and shifted to the right the concentration-response curve in the presence of $BaCl_2$ (30 μM) (Fig. 5A), 4-AP (1 mM) (Fig. 5B) and glibenclamide 10 μM (Fig. 5C). These findings suggest that K^+-channels activation type K_V, K_{ir}, K_{ATP} and mainly BK_{Ca}, plays an important role in the relaxant effect of 7-HC in mesenteric arteries.

3.4. In silico analysis

3.4.1. Pocket similarity analysis and druggability assessment

As 7-HC seems to bind to several K^+-channels, FTMap server was employed to identify clefts and pockets that are prone to bind organic solvent molecules (consensus sites), since these regions often match to the binding sites (Hall et al., 2012; Landon et al., 2009). Next, the information provided by this analysis lead to the classification of the putative binding pockets as druggable or borderline (Kozakov et al., 2015), if they are expected to bind compounds with nanomolar or micromolar affinity respectively (Fig. 6). The analysis of K_V tetrameric form, without the N-terminal or the transmembrane domains shows no druggable or borderline pockets. In contrast to that, a druggable pocket is predicted in the pore region of the transmembrane domain when 6 EBM 3D coordinates are employed (Fig. 6A). When this analysis is carried out with $K_{V1.2}$ N-terminal domain of chain B, a druggable ensemble of CSs (K_v DRG) is found (Fig. 6B). On the other hand, if the full-length K_V monomeric structure is taken into consideration, both the druggable (K_v_DRG2) and the borderline (K_v_BDR) pockets are found nearby the

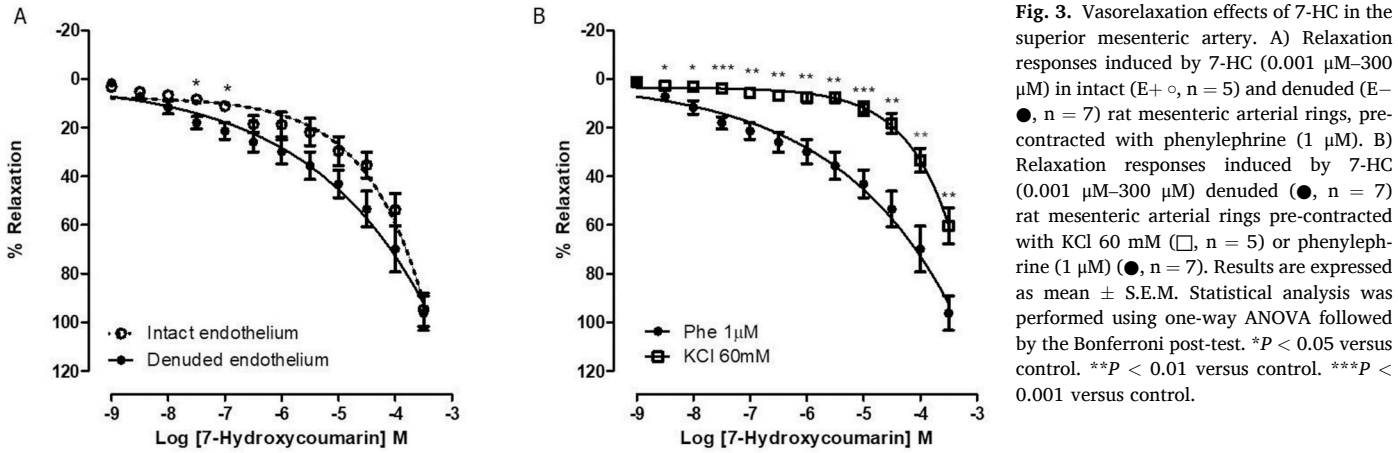

Fig. 3. Vasorelaxation effects of 7-HC in the superior mesenteric artery. A) Relaxation responses induced by 7-HC (0.001 μM–300 μM) in intact (E+ ○, n = 5) and denuded (E− ●, n = 7) rat mesenteric arterial rings, pre-contracted with phenylephrine (1 μM). B) Relaxation responses induced by 7-HC (0.001 μM–300 μM) denuded (●, n = 7) rat mesenteric arterial rings pre-contracted with KCl 60 mM (□, n = 5) or phenylephrine (1 μM) (●, n = 7). Results are expressed as mean ± S.E.M. Statistical analysis was performed using one-way ANOVA followed by the Bonferroni post-test. *$P < 0.05$ versus control. **$P < 0.01$ versus control. ***$P <$ 0.001 versus control.

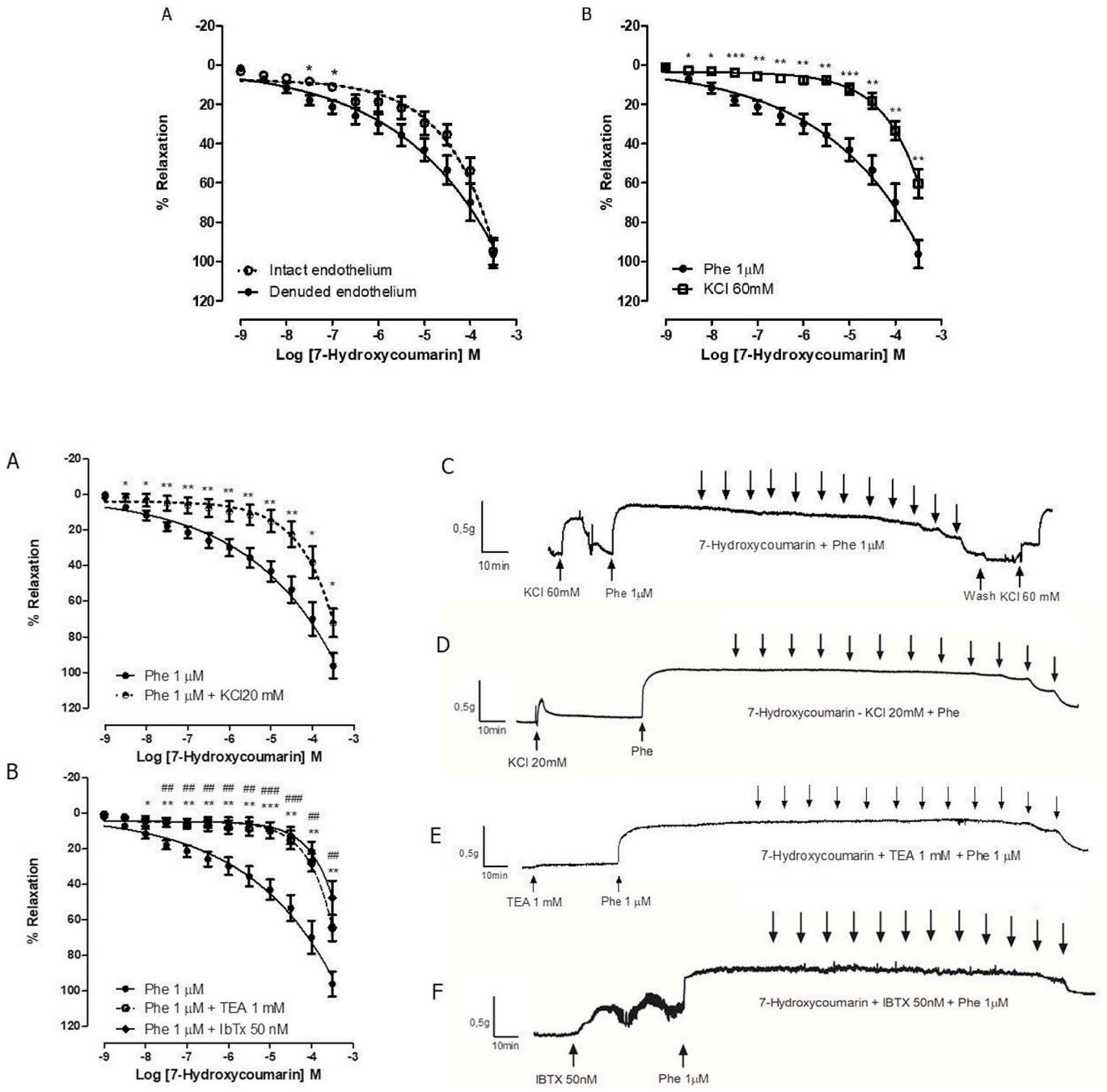

Fig. 4. Concentration-response curves (A and B) showing the relaxant effect of 7-HC (0.001 μM–300 μM in endothelium-denuded isolated mesenteric artery rings. Effects of Phe 1 μM (●, n = 7) or KCl 20 mM (▲, n = 5) (A) and tetraethylammonium 1 mM (○, n = 5) and iberiotoxin 50 nM (◆, n = 6) (B) on concentration–response curve of 7-HC in endothelium-denuded rat mesenteric arteries. Results are expressed as mean ± S.E.M. Representative original recordings of the effects of 7-HC on isolated mesenteric artery rings, pre-contracted with KCl 20 mM with phenylephrine (C), TEA 1 mM (D) or IbTx 50 nM (E). The arrows represent the time-course of the 7-HC administration (0.001 μM–300 μM). Statistical analysis was performed using unpaired Student's t-tests. $^{*}P < 0.05$ versus control. $^{**}P$ *or* $^{\#\#}P < 0.01$ versus control. $^{***}P$ *or* $^{\#\#\#}P < 0.001$ versus control.

TIM-barrel found in chain A (Fig. 6C). This result is not unexpected, since the N-terminal domain tetrameric form is not present in this structure.

A similar analysis for cytoplasmatic domain of K_{ir} in the monomeric form reveals two druggable ensembles of CSs (K_{ir}_DRG1 and K_{ir}_DRG2) close to each other (Fig. 6D). One of those pockets is predicted to be borderline if the K_{ir}'S tetrameric form is employed in the analysis.

The high sequence similarity between SUR1/Kir6.2 and the subtype found in the samples studied here (Principalli et al., 2015), makes it a suitable surrogate for this analysis. Considering that 6JB3 and 6PZA are among the highest resolution structure available, the druggable and borderline pockets for those structures were investigated (Fig. 6 – F–I). In both structures the CSs that lead to a druggable (6PZA - K_{ATP}_DRG) or a borderline (6JB3 – K_{ATP}_BDR) ensemble, are located in the inner-side of the transmembrane domain, however they are far apart.

Following a similar approach, only the two highest resolution BK_{Ca} structures available in PDB databank (3NAF and 6V22) were investigated. When the full-length tetrameric form of BK_{Ca} is mapped, no druggable or borderline ensemble is found. On the other hand, if only chain A is considered for the analysis, a small druggable ensemble of CSs

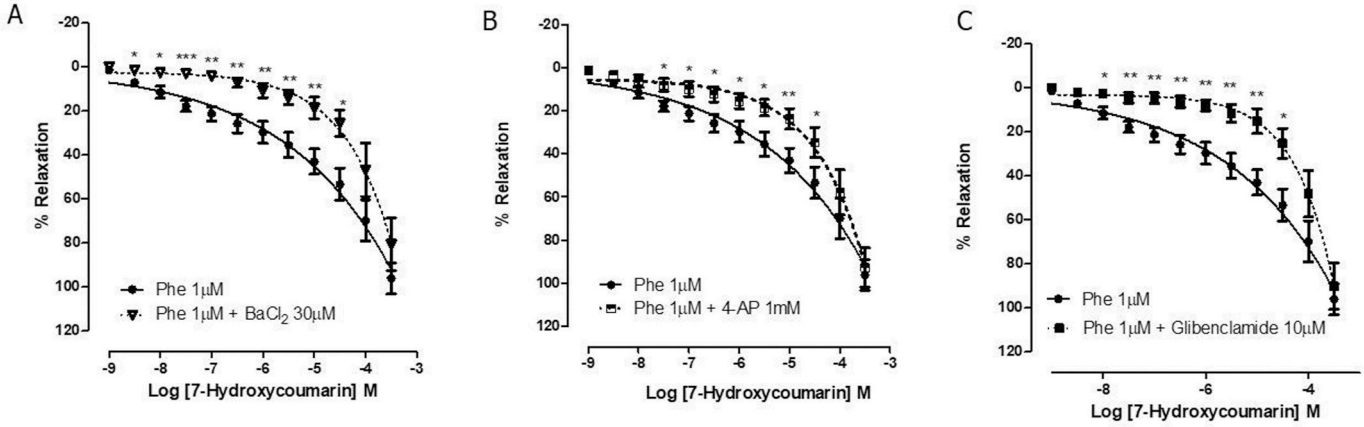

Fig. 5. Concentration-response curves showing the relaxant effect of 7-HC (0.001 μM–300 μM) on isolated endothelium-denuded mesenteric artery rings. Effects of $BaCl_2$ 30 μM (▼, n = 5) (A) and 4-AP 1 mM (□, n = 5) (B) and glibenclamide 10 μM (■, n = 6) (C) on concentration–response curve of 7-HC in endothelium-denuded rat mesenteric arteries. Results are expressed as mean ± S.E.M. $^{*}P < 0.05$ versus control. $^{**}P < 0.01$ versus control. $^{***}P < 0.001$ versus control.

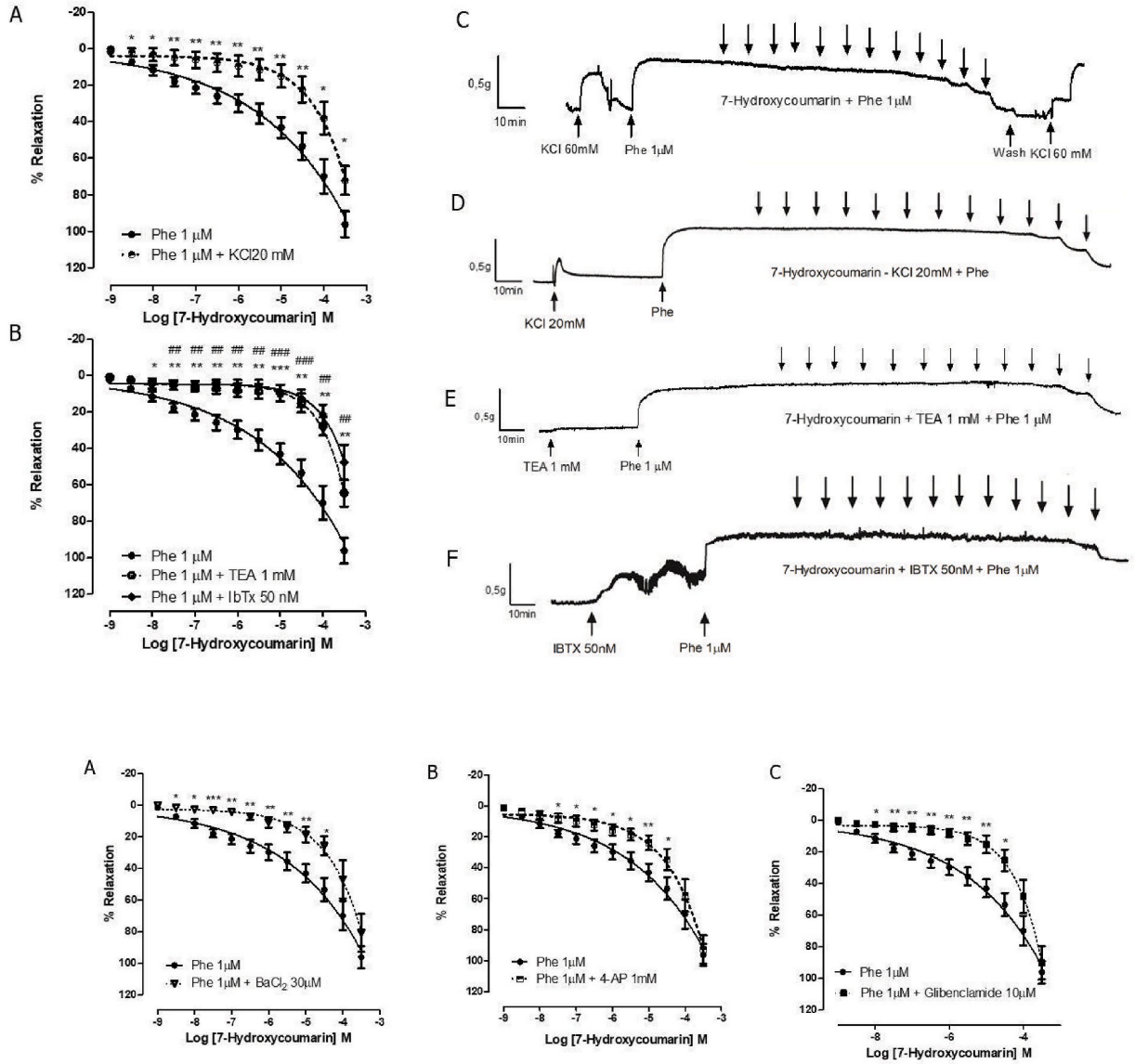

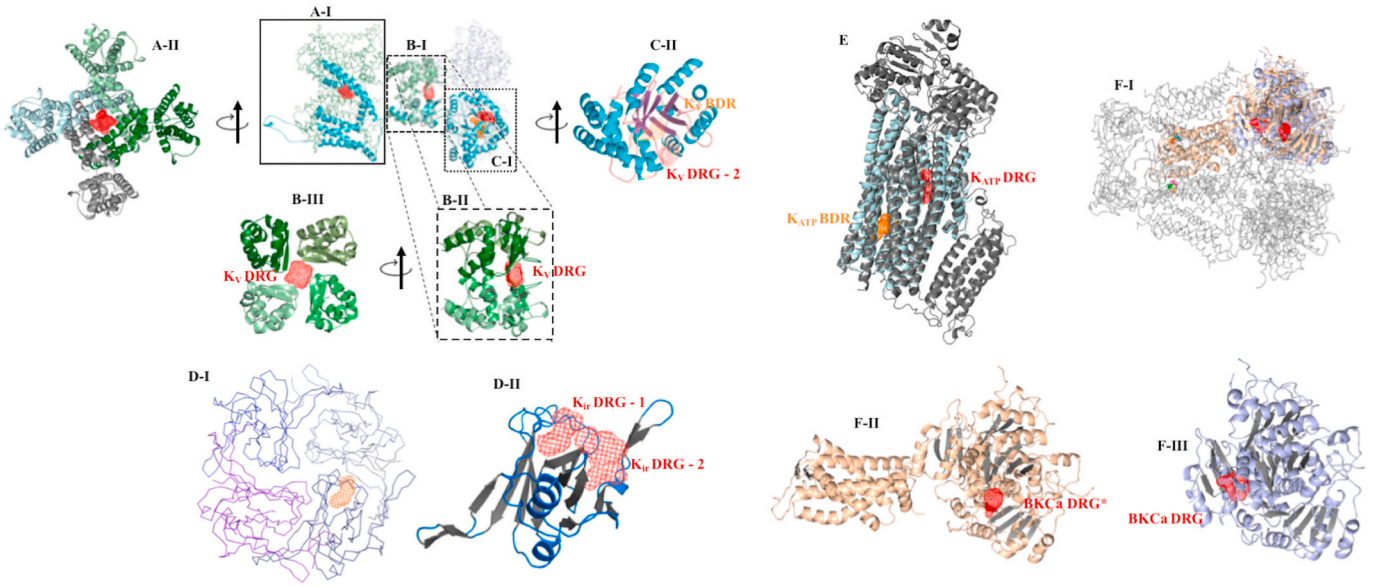

Fig. 6. Druggability assessment of potassium channels, according to FTMap criteria. Combinations of up to three consensus sites (CS), calculated with FTMap, were employed to find druggable (red mesh) and borderline (orange mesh) ensembles of CSs, as defined by Kozakov and co-workers (Kozakov et al., 2015). Side-view of druggable and borderline ensembles of CSs found in 6 EBM (A–I), 1QDV (B–I) and 3LUT (C–I) 6JB3 (E) and 6PZA (F-III); A-II) Top-view of druggable ensemble of CSs found in the pore region of Kv; B-II and B-III) Druggable ensembles of CSs found in the N-terminal domain of Kir(1QDV); C-II) Borderline and druggable ensemble of CSs found in 3LUT; D-I Borderline ensemble of CSs calculated for the tetrameric Kir structure (1U4F); D-II) Druggable ensembles of CSs predicted for Kir. F–I) Raw output from FTMap server for 6V22 (solvent molecules (sticks) are clustered in consensus sites) and the druggable ensembles of CSs identified when only chain A or the extra-cellular domain are employed in the analysis. F-II) Small druggable ensemble of CSs found in 6V22; F-III) Druggable ensemble of CSs predicted for 3NAF structure. The Protein structures in A-I, D-I, F–I (6V22 -tetramer) are depicted in ribbon, whereas the others are depicted in cartoon, colored according to chain ID, except for C-II, which is colored by secondary structure. (For interpretation of the references to color in this figure legend, the reader is referred to the Web version of this article.)

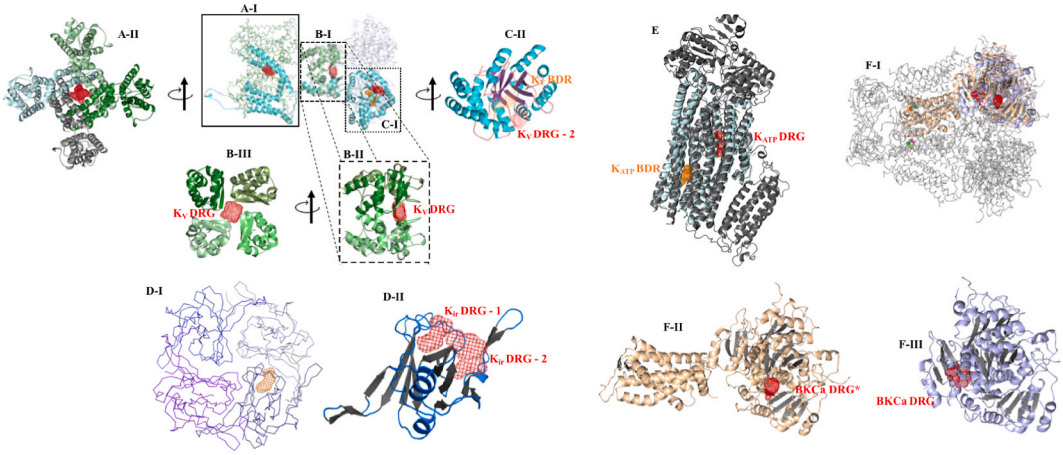

(BK_{Ca}_DRG*) is predicted, sandwiched between the beta-sheets (Fig. 6 – F-II and F-III).

3.4.2. *Molecular docking of 7-HC to potassium channels*

According to the pocket match server, Kv_BDR2 is somewhat similar to K_{ATP}_DRG, BK_{Ca}_DRG*, BK_{Ca}_DRG, and K_{ir}_DRG1, since their P-min score (Table 1S – supplementary material) is higher than 0.6 (Nagarajan and Chandra, 2013). The 3D coordinates of these sites are provided in the supplementary material. In order to evaluate if this pocket could be considered a common binding motif for 7-HC, this compound was docked to the above sites (Fig. 7), using SURFLEX default parameters.

Among the three best scored poses that provide a reasonable binding profile (i.e. no polar group buried in an apolar cleft), 7-HC is held into place, mostly, by hydrophobic interactions. However, the carbonyl group is expected to H-bonds to the side chain of either a basic (arginine) or a polar (glutamine) residue in all potassium binding sites, except for K_{ir}'s. Another striking difference is that K_{ir}'s binding site is the only one to allow the hydroxyl moiety at position 7 to H-bond. Despite that fact, 7-HC shows the highest H-bond network to BK_{Ca}'s binding site. In addition, the OH from 7-HC lies within dipole-dipole interaction to the side-chain of Ser 244 in K_v, Thr1242 and Arg 1300 in K_{ATP}, and Tyr1015 in BK_{Ca} (Fig. 7 and supplementary material) Hence, no polar groups are buried within hydrophobic pockets.

3.4.3. *Morphological similarity analysis*

The results from previous *in silico* analysis suggest that 7-HC might bind to BK_{Ca}, but one must consider that such result is biased by the pocket selected to carry out the molecular docking. Aiming at

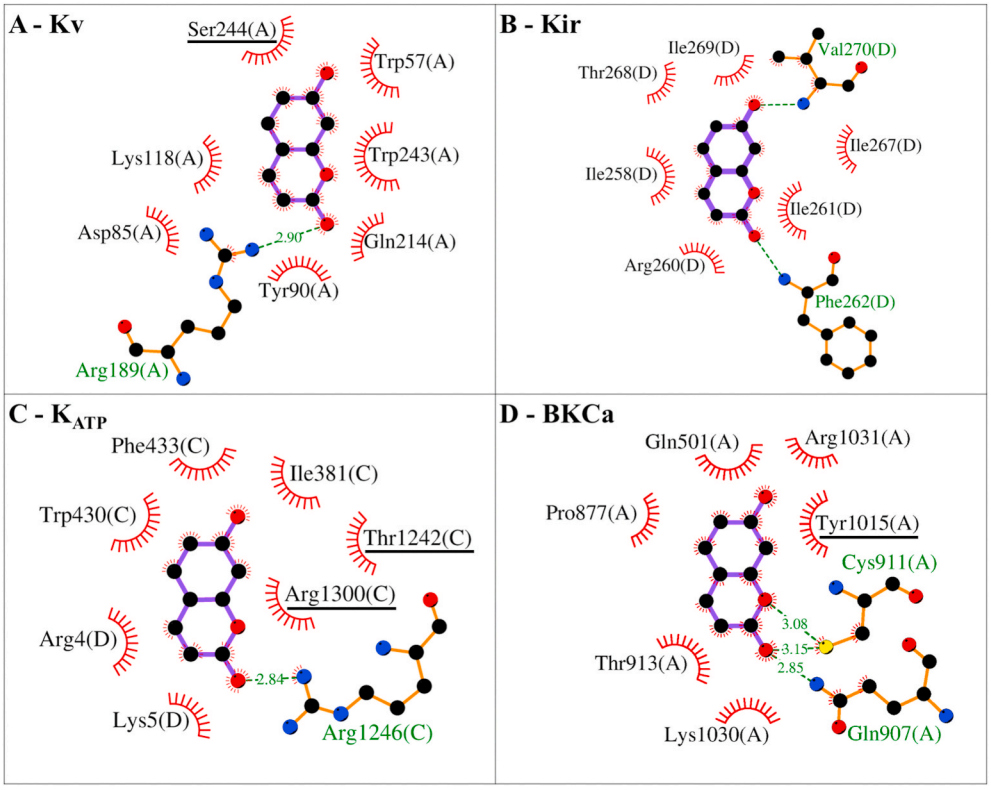

Fig. 7. 2D interaction profile of 7-HC's best docked poses to the putative common binding site found in potassium channels K_V (A), K_{ir} (B), K_{ATP} (C) and the second-best ranked pose to BK_{Ca} (D). Hydrophobic interactions are represented by spline curves that irradiate from the residues (named in black) or the atoms from 7-HC that take part in it. H-bonds are depicted in dashed lines, with distances measured in angstrom. Residues that perform dipole-dipole interaction to 7-HC are underscored. Atoms from the residues (named in green) that H-bond to 7-HC are color coded (carbon-black, nitrogen-blue; oxygen-red, sulfur-yellow). 7-HC atoms follow the same color scheme, but the bonds are depicted in violet. The chain identification is provided in parenthesis. (For interpretation of the references to color in this figure legend, the reader is referred to the Web version of this article.)

overcoming this limitation, an orthogonal ligand-based approach was employed. Thus, the morphological similarity of 7-HC was compared to non-peptide blockers of BK_{Ca} (Yu et al., 2016), using SURFLEX-SIM default parameters. According to this approach (Supplementary material – Fig. 1S) 7-HC is most similar to quinine (6.32) and ketamine (6.13) and least similar to tetrandine (3.70) and verapamil (4.43).

3.5. 7-HC inhibits Ca^{2+} influx

As shown in Fig. 8, the $CaCl_2$ concentration–response curve in the presence of 7-HC (3; 30 and 300 μM) in a depolarizing medium, was shifted to the right when compared with the control. The maximal contraction (E_{max}) of $CaCl_2$ was significantly attenuated to 60.9 ± 10.6% (P˂0.01 versus control, n = 5), only by the 300 μM concentration of 7-HC. These data indicate that part of the mechanism of action of 7-HC involves the reduction of Ca^{2+} influx.

3.6. Effect of SOCE inhibition on the relaxation induced by 7-HC

Fig. 9 shows that no changes were observed in the relaxation induced by 7-HC in the presence of the SOCE inhibitor SKF-96365. This result suggests that the inhibition of Ca^{2+} influx by SOCE is not involved in the vasorelaxation mechanism of 7-HC.

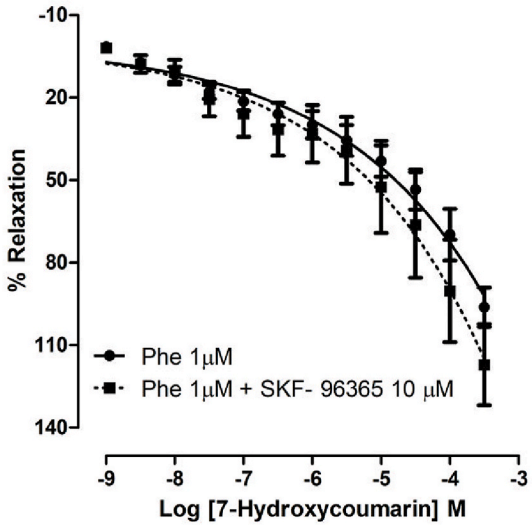

3.7. Effect of 7-HC on the mobilization of calcium from intracellular stores

The influence of 7-HC on the mobilization of Ca^{2+} from intracellular stores, through IP_3 receptors, was evaluated following Phe-induced contraction in a Ca^{2+}-free tyrode solution. 7-HC (30 μM and 300 μM) markedly reduced mesenteric ring vasoconstriction (41.7 ± 8.5%, 14.4 ± 5.2%, respectively) compared to control (100 ± 0), in a concentration-dependent manner (Fig. 10A/10 B/10C). Moreover, the effect of 7-HC on Ca^{2+} release from the internal store via ryanodine receptors was assessed by the caffeine induced contraction in a Ca^{2+}-free tyrode solution. 7-HC (30 μM and 300 μM) significantly decreased contraction (56.9 ± 11.6%, 54.9 ± 12.1%, respectively) compared to control (100 ±

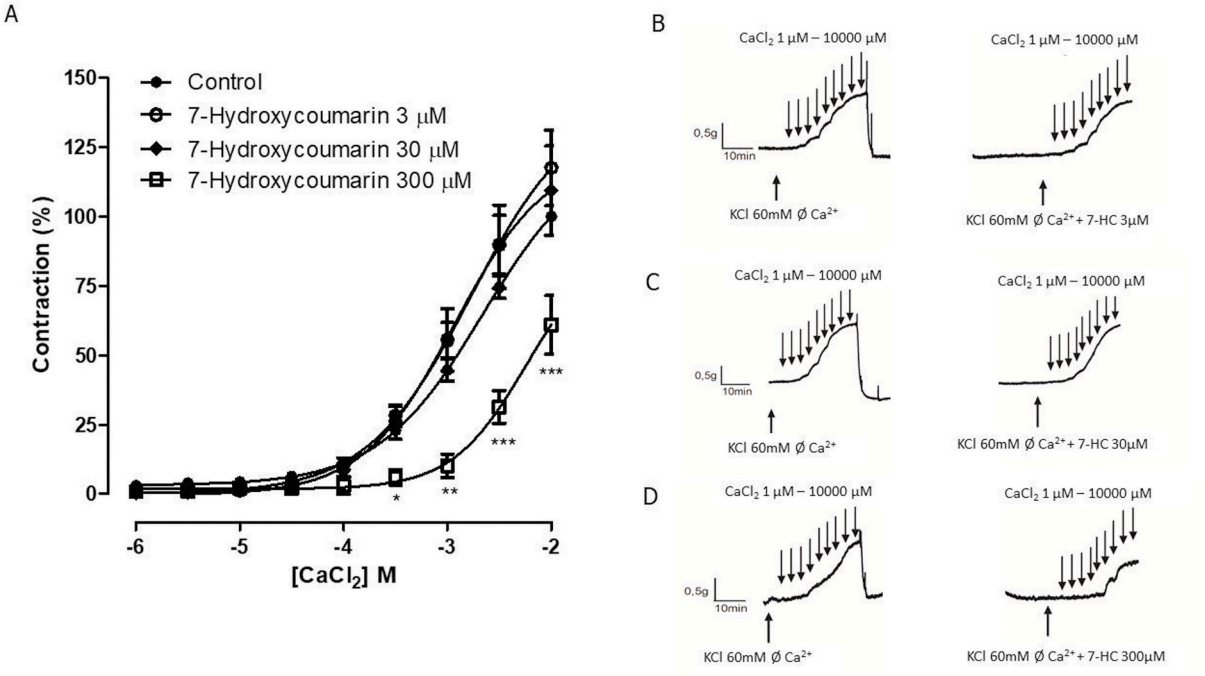

Fig. 8. Effect of 7-HC on Ca^{2+} influx. A) Concentration-response curve of $CaCl_2$ on rat mesenteric artery segments without endothelium, in the absence (●, n = 15) or in the presence of 7-HC (○, 3 μM, n = 5), (◆, 30 μM, n = 5) and (□, 300 μM, n = 5). Representative original recordings of the effects of 7-HC 3 μM (B), 30 μM (C) and 300 μM (D) on isolated mesenteric artery rings pre-incubated with calcium-free KCl 60 mM. The arrows represent the time-course of the Ca^{2+} administration (1 μM–10,000 μM). Statistical analysis was performed using unpaired Student's t-tests. *$P < 0.05$, **$P < 0.01$ and ***$P < 0.001$ versus control.

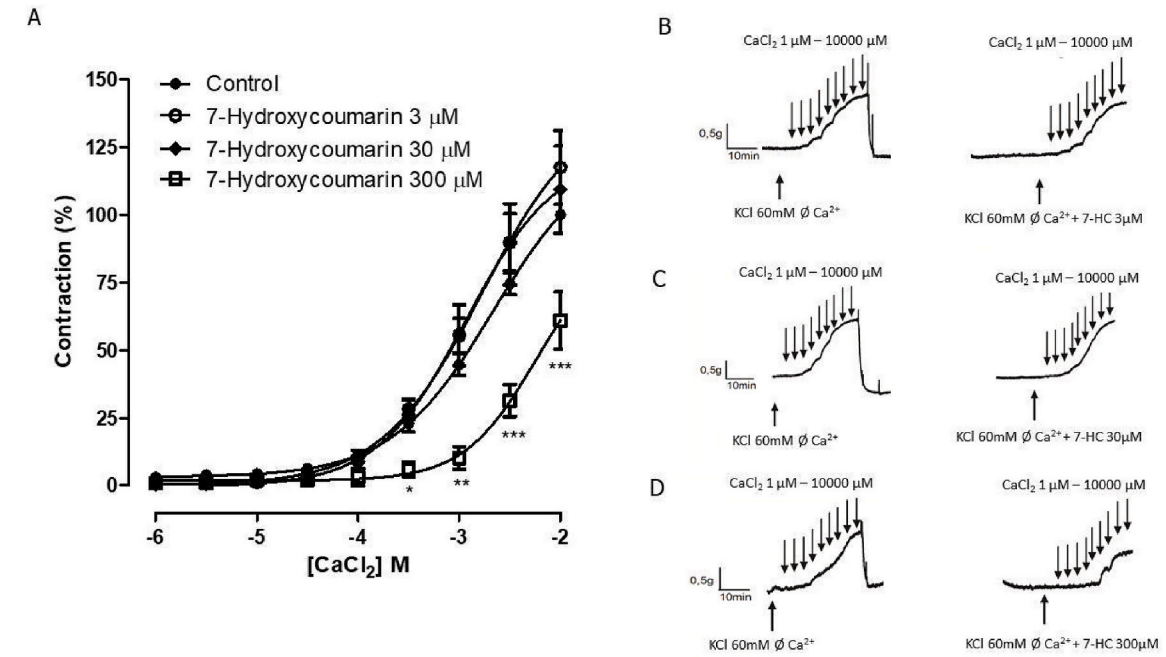

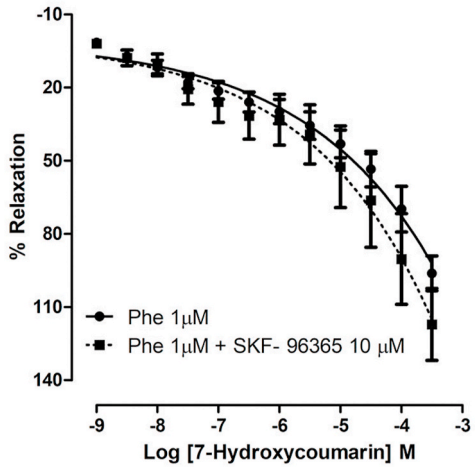

Fig. 9. Vasorelaxant effect of 7-HC in the presence of SOCE inhibition. Relaxation responses induced by 7-HC (0.001 μM–300 μM) on the isolated endothelium-denuded mesenteric artery rings, pre-contracted with phenylephrine, in the presence or absence of SKF-96365 (10 μM). Results are expressed as mean ± S.E.M. (n = 8). Statistical analysis was performed using unpaired Student's *t* tests.

0), in a concentration-independent manner (Fig. 10D/10 E/10 F). These data suggest that the mechanism of action of 7-HC involves the reduction of Ca^{2+} release from the intracellular store via IP_3 receptors and ryanodine receptors.

4. Discussion

Our results suggest that 7-HC is capable of inducing an endothelium-independent vasorelaxant effect, which likely involves the activation of potassium channels (K_v, K_{ir}, K_{ATP} and BK_{Ca}), reduction of calcium influx and intracellular calcium mobilization. To the best of our knowledge, this is the first work that shows this vasorelaxant effect of 7-HC and its proposed mechanisms of action.

In order to investigate the direct effect of 7-HC in the vasculature, independent of neuro-humoral influences, experiments were performed in isolated rat mesenteric artery rings with and without endothelium, pre-contracted with phenylephrine (1 μM), an α1-adrenergic agonist. Under this controlled condition, 7-HC (0.001 μM–300 μM) induced a pronounced relaxation effect in a concentration dependent manner. Although the endothelium controls vascular reactivity (and blood pressure) by releasing paracrine signaling molecules (Godo and Shimokawa, 2017), the influence of endothelium-derived vasoactive factors in response to 7-HC appeared to be less relevant. Thus, the subsequent experiments were carried out to investigate the 7-HC endothelium-independent vasorelaxation mechanisms.

7-HC was found to be non-toxic in cardiomyocytes at the concentrations tested and in a reversibility of vascular contractility trial, following cumulative addition of 7-HC, we observed that tissue contractility was maintained even after the removal of 7-HC from tissue bath solution, suggesting that 7-HC has no irreversible actions on contractile machinery, nor possible toxic effects on vascular myocyte, at least at the concentrations tested (data not shown), corroborating with the cytotoxicity assessment test. In addition, Cruz et al. (2020) evaluated the acute oral toxicity of 7-HC in mice. The animals were observed continuously after administration of 7-HC (50, 100 and 200 mg/kg) to assess any changes in autonomy, behavior, number of deaths and general neurological profiles. There were no changes in the number of deaths, daily body weight, behaviors or macroscopic changes in the vital organs after the treatment of animals with 7-HC, demonstrating the absence of toxic effect. This result corroborates the study by Muthu et al. (2013) who showed that no signs of toxicity were observed in rats treated with 7-HC (Muthu et al., 2013). Furthermore, it is important to describe that 7-HC did not alter resting tone of the arterial smooth muscle, following cumulative administration. This result suggests that 7-HC does not evoke vasorelaxant or vasoconstrictor response at basal tone. In order to exert its vasorelaxant effect, it is essential that the mesenteric artery rings are pre-contracted.

The elevated vascular tone, observed in human hypertension and in several experimental hypertension models, have involved alterations in Ca^{2+} and/or K^+ channel expression and function in VSMC, contributing to cardiovascular pathology. Several families of Ca^{2+} and K^+ channels are expressed in VSMC and three types of channels have been reported to be altered in animal models of hypertension: Ca^{2+} type L channels

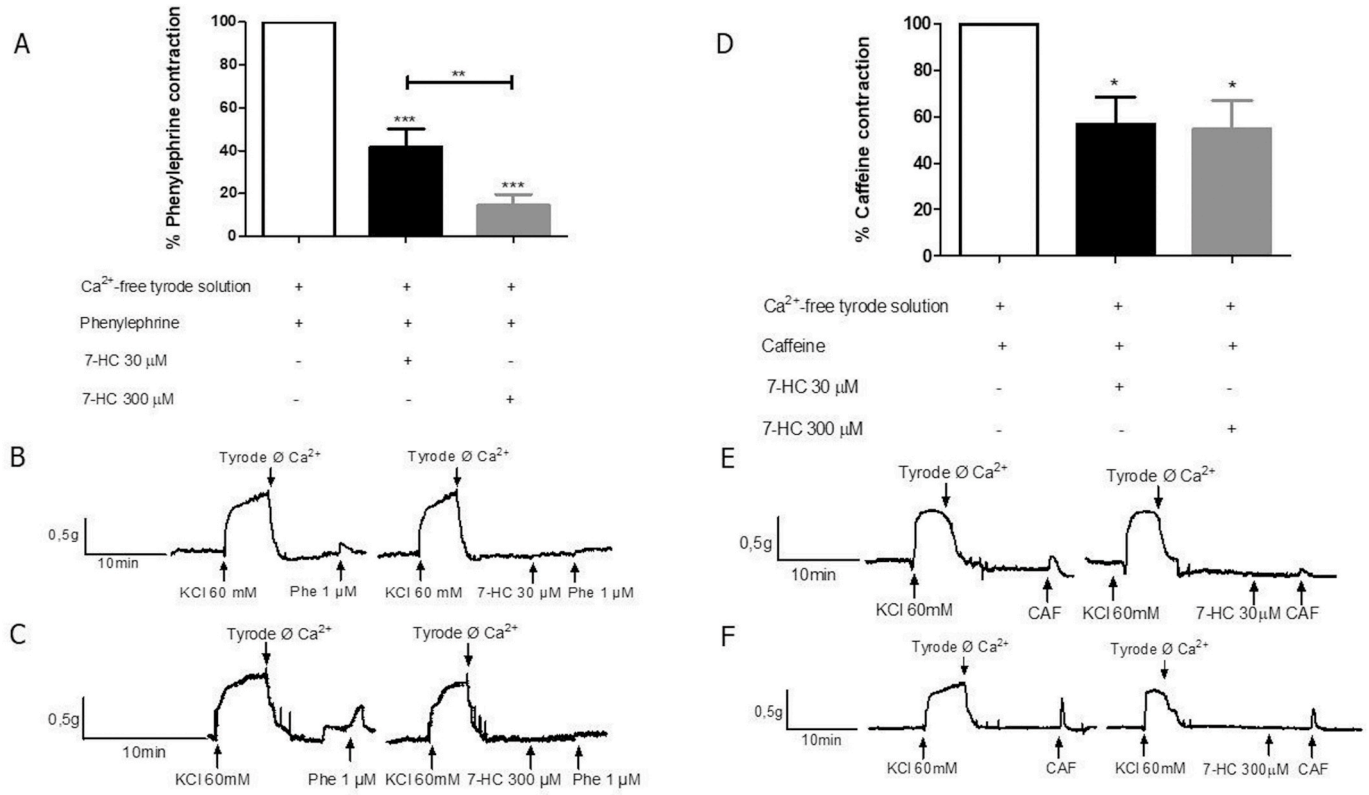

Fig. 10. Effect of 7-HC on intracellular Ca^{2+}. Effect of 7-HC (30 µM and 300 µM) on the mobilization of Ca^{2+} from phenylephrine (A) and caffeine (D) sensitive intracellular stocks, in Ca^{2+}-free tyrode solution. Representative original recordings of the effects of 7-HC 30 µM and 300 µM on isolated mesenteric artery rings incubated with phenylephrine 1 µM (B and C) or caffeine 20 mM (E and F) in a calcium-free solution. Results are expressed as mean ± S.E.M. Statistical analysis was performed using one-way ANOVA followed by the Bonferroni post-test.

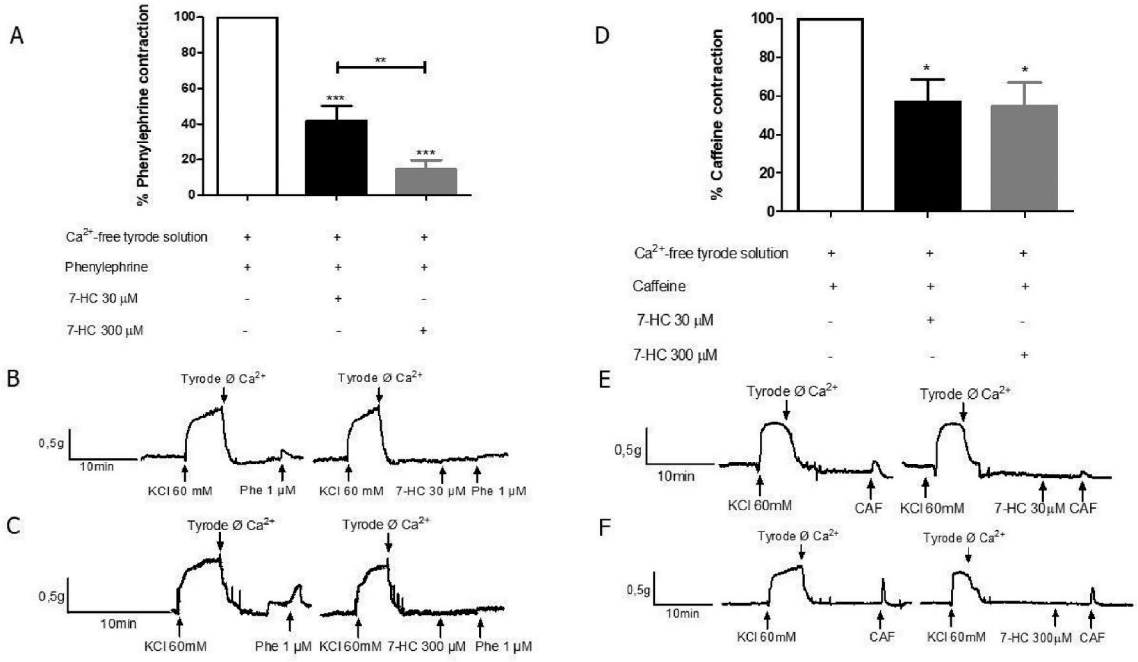

($Ca_V1.2$) (Tajada et al., 2013), voltage-dependent K^+ channels (K_V) (Cox and Rusch, 2002), and the broad conductance Ca^{2+} activated K^+ channels (BK_{Ca}) (Yang et al., 2013; Zhang et al., 2018). Thus, the results found in this study are relevant, considering that there is increased vascular tone in the hypertensive state and, thus, 7-HC would likely have a more pronounced effect in human hypertension than in the normotensive condition. However, additional studies should be performed to address this hypothesis.

To evaluate the involvement of K^+ channels in 7-HC-mediated vasorelaxant response, experiments were performed in endothelium-denuded arterial rings, incubated with 20 mM KCl. The increase in extracellular K^+ concentration (from 4 to 20 mM) partially decreased membrane efflux of K^+, resulting in a reduced electrochemical gradient, which affects vasorelaxation related to K^+ channels activation (Brochet and Langton, 2006). Under these conditions, the response to 7-HC was significantly attenuated, which was also observed when rings were exposed to 60 mM KCl, suggesting the participation of K^+ channels in 7-HC induced vasorelaxation. Thus, the involvement and activation of distinct types of K^+ channels in 7-HC induced vasorelaxation was investigated.

BK_{Ca} channels are abundantly expressed in vascular smooth muscle and they are an important controller of cellular depolarization and contraction in these tissues (Brayden and Nelson, 1992, Nelson and Quayle, 1995, Dogan et al., 2019). It is well established that BK_{Ca} channels are highly expressed in vascular smooth muscles (Latorre et al., 2017). In order to probe the involvement of BK_{Ca} channels in the 7-HC response, preparations were pretreated with TEA (1 mM), a blocker of BK_{Ca} channels or iberiotoxin 50 nM, a selective a blocker of the BK_{Ca} and the vasorelaxant response induced by increasing concentrations of 7-HC was significantly attenuated, suggesting the participation of BK_{Ca} channels, at least at these concentrations.

The presence of the K_{ATP} channel blocker, Glib (10 μM), or a K_V channels blocker, 4-AP (1 mM), on the mesenteric rings, shifted the concentration–response curve for 7-HC to the right. The same response occurred in rings preincubated with $BaCl_2$ (30 μM), a K_{ir} channels blocker, suggesting that K_{ATP}, K_V, and K_{ir} channels accounts for the vasorelaxant action attributed to 7-HC, at least in part. The lack of electrophysiological data for this investigation is a major limitation of the study, however, additional experiments using an electrophysiological approach, specially One-channel cell-attached patch-clamp measurements, should be performed to confirm the hypothesis that 7-HC induces the opening of K^+ channels, especially BK_{Ca}. Besides that, would be helpful to examine the effects of this molecule in blood vessels using glass microelectrode and determine its electrophysiological effects on smooth muscle cells.

An alternative approach relies on the use of molecular modeling tools to further probe this hypothesis. In fact, computational analysis were instrumental to explore putative binding sites for paxilline to BK_{Ca} (Zhou et al., 2019), molecular docking studies have been employed to evaluate the binding of a berberine derivative to Ca_v and K_v (Hu et al., 2020), molecular dynamic simulations have shed light on the binding profile of tertiapin, a peptide find in the venon from *Apis mellifera*, to K_{ir} (Patel et al., 2020). All these studies are supported by sound experimental data, once molecular modeling results may be biased by several user-defined parameters (Jain, 2008). One of the most obvious parameters that has a high impact on docking performance and biological relevance is the definition of the putative binding site. In this study, a non-biased protocol, which relies on the virtual solvent mapping approach, was employed to identify pockets and crevices that might allow 7-HC to bind with micromolar or nanomolar affinity. The comparison of those pockets hints that K_{ATP}, BK_{Ca}, K_v, and K_{ir} might have a common allosteric site that shares moderate similarity among those potassium channel and that may be the biological target of 7-HC. In agreement with this hypothesis the docking studies demonstrated that 7-HC might bind to this pocket, since its polar and apolar interaction networks are well-satisfied. Although this result corroborates the experimental results reported here, Singh and coworkers propose a different binding site in BK_{Ca} for chromeno-coumarin derivatives that have vasorelaxant effects (Singh et al., 2020). Hence, further experiments are required to shed light on this subject. To provide further insights into 7-HC putative binding site in BK_{Ca}, morphological similarity analysis was carried out, using compounds that bind to BK_{Ca}. The vast chemical diversity among the BK_{Ca} blockers employed in such analysis suggest that they do not bind to the same pocket. This analysis suggests that 7-HC's putative binding site to BK_{Ca} is more similar to quinine's or ketamine's, than tetrandine's and verapamil's.

In addition, we evaluated whether vasorelaxation induced by 7-HC is associated with the inhibition of Ca^{2+} influx, since it has been described that vascular tone induced by an increase in extracellular K^+ occurs due to the opening of voltage-gated calcium channels and, taking into account that although attenuated, 7-HC was able to reduce the contraction induced by KCl 60 mM. Therefore, there is the possibility that 7-HC interferes with calcium influx in the VSMC. Only 7-HC at 100 μM reduced the Ca^{2+}-mediated vasoconstriction in mesenteric rings lacking endothelium that were pre-incubated with a high K^+ solution (60 mM KCl) nominally, without Ca^{2+}. We speculate that this response may be the result of K^+ efflux from VSMC caused by K^+ channel activation, leading to plasma membrane hyperpolarization and Ca^{2+} channel closure. This suggests that 7-HC preferably leads to K^+ efflux and at higher concentrations may, in a nonspecific manner, reduce Ca^{2+} influx. Furthermore, experiments were performed to assess the involvement of SOCE in relaxation induced by 7-HC, using the non-specific SOCE inhibitor, SKF-96365. The results indicate that the 7-HC-mediated relaxation was similar in the presence and absence of SKF-96365, indicating a lack of inhibition of Ca^{2+} entry through SKF-sensitive channels by 7-HC. Interestingly, our results corroborate with the study of Zhang and coworkers (2010), that demonstrated that in isolated artery rings, furanocoumarin imperatorin potentially caused endothelium-independent relaxation of rat small mesenteric artery not by inhibiting SOCE in VSMCs (Zhang et al., 2010).

Next, another experimental protocol was performed to assess whether the effect of 7-HC could reduce mobilization of calcium from intracellular stores. Inositol 1,4,5-trisphosphate receptors (IP_3 receptors) and ryanodine receptors are Ca^{2+} release channels on the endo/sarcoplasmic reticulum (ER/SR) (Go et al., 1995; Rossi and Taylor, 2018). In addition, to evaluate whether the vasorelaxant effect of 7-HC could involve inhibition of calcium mobilization from intracellular stores, via ryanodine receptors and IP_3 receptors, arterial rings were studied in a Ca^{2+}-free tyrode solution in the presence of phenylephrine, utilized to stimulate IP_3 receptors, or by caffeine, used to activate ryanodine receptors. Under these conditions, 7-HC markedly decreased mobilization of calcium from intracellular stores, via IP_3 receptors, in a concentration-dependent manner. Also, 7-HC reduced Ca^{2+} release from the internal store via ryanodine receptors, in a concentration-independent manner. These results indicate that the vasorelaxant response of 7-HC may also involve, at least in part, the inhibition of Ca^{2+} release from the internal store through IP_3 receptors and ryanodine receptors, leading to a decrease in $[Ca^{2+}]_i$.

One limitation of this study was that it was not possible to determine whether 7-HC reduced Ca^{2+} release from the sarcoplasmic reticulum by direct action on the ryanodine receptors and IP_3 receptors or if the reduced contractions induced by Ca^{2+} release from the reticulum induced by 7- HC, would be a result of the activation of K^+ channels, followed by the Ca^{2+} influx reduction in the VSMC, leading to a lower calcium-induced calcium release response. Additional studies using confocal microscopy may elucidate this aspect of the mechanism of action involved in 7-HC responses.

5. Conclusions

Taken together, these results demonstrate that 7-HC induced vasorelaxation, most likely through BK_{Ca} channels activation, on the smooth muscle from rat superior mesenteric artery. Additionally, 7-HC is capable of attenuating calcium influx, which leads to reduction of intracellular calcium mobilization. These collective results suggest that 7-HC is a promising lead compound with direct vascular activity for drug development to treat hypertension. However, further studies will be necessary to investigate the actions of 7-HC on cardiac tissue.

CRediT authorship contribution statement

Quiara Lovatti Alves: Data curation, Formal analysis, Investigation, Methodology, Writing - original draft. **Raiana dos Anjos Moraes:** Data curation, Formal analysis, Methodology. **Thamires Quadros Froes:** Data curation, Formal analysis, Methodology. **Marcelo Santos Castilho:** Formal analysis, Methodology, Writing - review & editing. **Rodrigo Santos Aquino de Araújo:** Formal analysis, Methodology. **José Maria Barbosa-Filho:** Formal analysis, Methodology, Writing - review & editing. **Cássio Santana Meira:** Formal analysis, Methodology. **Milena Botelho Pereira Soares:** Formal analysis, Methodology. **Darízy Flávia Silva:** Conceptualization, Formal analysis, Funding acquisition, Project administration, Writing - review & editing.

Declaration of competing interest

The authors declare that there are no conflicts of interest. The founding sponsors had no role in the design of the study; in the collection, analysis, or interpretation of data; in the writing of the manuscript, nor in the decision to publish the results.

Acknowledgments

This study was funded by grants from National Council for Scientific and Technological Development (CNPq) 306106/2017–5 and Coordination for the Improvement of Higher Education Personnel (CAPES) - Finance Code 001. We acknowledge the computational support from SCC1 (Boston University) and technical support from Pedro S. Lacerda.

Appendix A. Supplementary data

Supplementary data to this article can be found online at https://doi.org/10.1016/j.ejphar.2020.173525.

References

Baccard, Mechiche, Nazeyrollas, Manot, Lamiable, Devillier, Millart, 2000. Effects of 7-hydroxycoumarin (umbelliferone) on isolated perfused and ischemic-reperfused rat heart. Arzneimittelforschung 50, 890–896. https://doi.org/10.1055/s-0031-1300317.

Brayden, J.E., Nelson, M.T., 1992. Regulation of arterial tone by activation of calcium-dependent potassium channels. Science 256, 532–535. https://doi.org/10.1126/science.1373909.

Brochet, D.X.P., Langton, P.D., 2006. Dual effect of initial [K] on vascular tone in rat mesenteric arteries. Pflugers Arch. Eur. J. Physiol. 453, 33–41. https://doi.org/10.1007/s00424-006-0106-1.

Chen, T., Zhu, J., Zhang, C., Huo, K., Fei, Z., Jiang, X.F., 2013. Protective effects of SKF-96365, a non-specific inhibitor of SOCE, against MPP+-Induced cytotoxicity in PC12 cells: potential role of Homer 1. PloS One 8. https://doi.org/10.1371/journal.pone.0055601.

Cox, R.H., Rusch, N.J., 2002. New expression profiles of voltage-gated ion channels in arteries exposed to high blood pressure. Microcirculation 9, 243–257. https://doi.org/10.1038/sj.mn.7800140.

Cruz, L.F., Figueiredo de, G.F., Pedro, L.P., Amorin, Y.M., Andrade, J.T., Passos, T.F., Rodrigues, F.F., Souza, I.L.A., Gonçalves, T.P.R., dos Santos Lima, L.A.R., Ferreira, J. M.S., Araújo de, M.G.F., 2020. Umbelliferone (7-hydroxycoumarin): a non-toxic antidiarrheal and antiulcerogenic coumarin. Biomed. Pharmacother. 129, 110432. https://doi.org/10.1016/j.biopha.2020.110432.

De Almeida Barros, T.A., De Freitas, L.A.R., Filho, J.M.B., Nunes, X.P., Giulietti, A.M., De Souza, G.E., Dos Santos, R.R., Soares, M.B.P., Villarreal, C.F., 2010. Antinociceptive and anti-inflammatory properties of 7-hydroxycoumarin in experimental animal models: potential therapeutic for the control of inflammatory chronic pain. J. Pharm. Pharmacol. 62, 205–213. https://doi.org/10.1211/jpp.62.02.0008.

de Araújo, R.S.A., Guerra, F.Q.S., Lima de, E.O., de Simone, C.A., Tavares, J.F., Scotti, L., Scotti, M.T., de Aquino, T.M., de Moura, R.O., Mendonça, F.J.B., Barbosa-Filho, J.M., 2013. Synthesis, structure-activity relationships (SAR) and in silico studies of coumarin derivatives with antifungal activity. Int. J. Mol. Sci. 14, 1293–1309. https://doi.org/10.3390/ijms14011293.

De Lima, F.O., Nonato, F.R., Couto, R.D., Barbosa Filho, J.M., Nunes, X.P., Ribeiro Dos Santos, R., Soares, M.B.P., Villarreal, C.F., 2011. Mechanisms involved in the antinociceptive effects of 7-hydroxycoumarin. J. Nat. Prod. 74, 596–602. https://doi.org/10.1021/np100621c.

Dogan, M.F., Yildiz, O., Arslan, S.O., Ulusoy, K.G., 2019. Potassium channels in vascular smooth muscle: a pathophysiological and pharmacological perspective. Fundam. Clin. Pharmacol. 33, 504–523. https://doi.org/10.1111/fcp.12461.

Frieden, M., Sollini, M., Bény, J.L., 1999. Substance P and bradykinin activate different types of K(Ca) currents to hyperpolarize cultured porcine coronary artery endothelial cells. J. Physiol. 519, 361–371. https://doi.org/10.1111/j.1469-7793.1999.0361m.x.

Go, L.O., Moschella, M.C., Watras, J., Handa, K.K., Fyfe, B.S., Marks, A.R., 1995. Differential regulation of two types of intracellular calcium release channels during end-stage heart failure. J. Clin. Invest. 95, 888–894. https://doi.org/10.1172/JCI117739.

Godo, S., Shimokawa, H., 2017. Endothelial functions. Arterioscler. Thromb. Vasc. Biol. 37, e108–e114. https://doi.org/10.1161/ATVBAHA.117.309813.

Hall, D.R., Kozakov, D., Vajda, S., 2012. Analysis of protein binding sites by computational solvent mapping. Comminution 13–27. https://doi.org/10.1007/978-1-61779-465-0_2.

He, J.Y., Zhang, W., He, L.C., Cao, Y.X., 2007. Imperatorin induces vasodilatation possibly via inhibiting voltage dependent calcium channel and receptor-mediated Ca2+ influx and release. Eur. J. Pharmacol. 573, 170–175. https://doi.org/10.1016/j.ejphar.2007.06.043.

Hotwani, K., Baliga, S., Sharma, K., 2014. Phytochemistry: use of medicinal plants. J. Compl. Integr. Med. 11, 233–251. https://doi.org/10.1515/jcim-2013-0015.

Hu, H., Zhou, S., Sun, Xiaodong, Xue, Y., Yan, L., Sun, Xuanxuan, Lei, M., Li, J., Zeng, X., Hao, L., 2020. A potent antiarrhythmic drug N -methyl berbamine extends the action potential through inhibiting both calcium and potassium currents. J. Pharmacol. Sci. 142, 131–139. https://doi.org/10.1016/j.jphs.2019.12.008.

Insuk, S.O., Chae, M.R., Choi, J.W., Yang, D.K., Sim, J.H., Lee, S.W., 2003. Molecular basis and characteristics of KATP channel in human corporal smooth muscle cells. Int. J. Impot. Res. 15, 258–266. https://doi.org/10.1038/sj.ijir.3901013.

Jagadeesh, G.S., Nagoor Meeran, M.F., Selvaraj, P., 2016. Protective effects of 7-hydroxycoumarin on dyslipidemia and cardiac hypertrophy in isoproterenol-induced myocardial infarction in rats. J. Biochem. Mol. Toxicol. 30, 120–127. https://doi.org/10.1002/jbt.21770.

Jain, A.N., 2008. Bias, reporting, and sharing: computational evaluations of docking methods. J. Comput. Aided Mol. Des. 22, 201–212. https://doi.org/10.1007/s10822-007-9151-x.

Jain, A.N., 2007. Surflex-Dock 2.1: robust performance from ligand energetic modeling, ring flexibility, and knowledge-based search. J. Comput. Aided Mol. Des. 21, 281–306. https://doi.org/10.1007/s10822-007-9114-2.

Kawabata, A., Kubo, S., Nakaya, Y., Ishiki, T., Kuroda, R., Sekiguchi, F., Kawao, N., Nishikawa, H., 2004. Distinct roles for protease-activated receptors 1 and 2 in vasomotor modulation in rat superior mesenteric artery. Cardiovasc. Res. 61, 683–692. https://doi.org/10.1016/j.cardiores.2003.11.030.

Kjeldsen, S.E., 2018. Hypertension and cardiovascular risk: general aspects. Pharmacol. Res. 129, 95–99. https://doi.org/10.1016/j.phrs.2017.11.003.

Kozakov, D., Hall, D.R., Napoleon, R.L., Yueh, C., Whitty, A., Vajda, S., 2015. New frontiers in druggability. J. Med. Chem. 58, 9063–9088. https://doi.org/10.1021/acs.jmedchem.5b00586.

Landon, M.R., Lieberman, R.L., Hoang, Q.Q., Ju, S., Caaveiro, J.M.M., Orwig, S.D., Kozakov, D., Brenke, R., Chuang, G.Y., Beglov, D., Vajda, S., Petsko, G.A., Ringe, D., 2009. Detection of ligand binding hot spots on protein surfaces via fragment-based methods: application to DJ-1 and glucocerebrosidase. J. Comput. Aided Mol. Des. 23, 491–500. https://doi.org/10.1007/s10822-009-9283-2.

Langton, P.D., Nelson, M.T., Huang, Y., Standen, N.B., 1991. Block of calcium-activated potassium channels in mammalian arterial myocytes by tetraethylammonium ions. Am. J. Physiol. Heart Circ. Physiol. 260 https://doi.org/10.1152/ajpheart.1991.260.3.h927.

Latorre, R., Castillo, K., Carrasquel-Ursulaez, W., Sepulveda, R.V., Gonzalez-Nilo, F., Gonzalez, C., Alvarez, O., 2017. Molecular determinants of BK channel functional diversity and functioning. Physiol. Rev. 97, 39–87. https://doi.org/10.1152/physrev.00001.2016.

Lemmich, J., Havelund, S., Thastrup, O., 1983. Dihydrofurocoumarin glucosides from Angelica archangelica and Angelica silvestris. Phytochemistry 22, 553–555. https://doi.org/10.1016/0031-9422(83)83044-1.

Markham, M.-J., Dog, T.L., 2013. Dietary supplements and hemostasis. In: Consultative Hemostasis and Thrombosis. Elsevier, pp. 595–600. https://doi.org/10.1016/B978-1-4557-2296-9.00032-4.

Muthu, R., Thangavel, P., Selvaraj, N., Ramalingam, R., Vaiyapuri, M., 2013. Synergistic and individual effects of umbelliferone with 5-flurouracil on the status of lipid peroxidation and antioxidant defense against 1, 2-dimethylhydrazine induced rat colon carcinogenesis. Biomed. Prev. Nutr. 3, 74–82. https://doi.org/10.1016/j.bionut.2012.10.011.

Nagarajan, D., Chandra, N., 2013. PocketMatch (version 2.0): a parallel algorithm for the detection of structural similarities between protein ligand binding-sites. In: 2013 Natl. Conf. Parallel Comput. Technol. PARCOMPTECH 2013. https://doi.org/10.1109/ParCompTech.2013.6621397, 0–5.

Nelson, M.T., Quayle, J.M., 1995. Physiological roles and properties of potassium channels in arterial smooth muscle. Am. J. Physiol. 268, C799–C822. https://doi.org/10.1152/ajpcell.1995.268.4.C799.

Oliveira, E.J., Romero, M.A., Silva, M.S., Silva, B.A., Medeiros, I.A., 2001. Intracellular calcium mobilization as a target for the spasmolytic action of scopoletin. Planta Med. 67, 605–608. https://doi.org/10.1055/s-2001-17355.

Patel, D., Kuyucak, S., Doupnik, C.A., 2020. Structural determinants mediating tertiapin block of neuronal Kir 3.2 channels. Biochemistry 59, 836–850. https://doi.org/10.1021/acs.biochem.9b01098.

Petrovska, B.B., 2012. Historical review of medicinal plants' usage. Pharm. Rev. 6, 1–5. https://doi.org/10.4103/0973-7847.95849.

Principalli, M.A., Dupuis, J.P., Moreau, C.J., Vivaudou, M., Revilloud, J., 2015. Kir6.2 activation by sulfonylurea receptors: a different mechanism of action for SUR1 and

SUR2A subunits via the same residues. Phys. Rep. 3, 1–9. https://doi.org/10.14814/phy2.12533.
RA, L., MB, S., 2011. LigPlot+: multiple ligand-protein interaction diagrams for drug discovery. J. Chem. Inf. Model. 51, 2778–2786.
Rossi, A.M., Taylor, C.W., 2018. IP3 receptors - lessons from analyses ex cellular. J. Cell Sci. 132 https://doi.org/10.1242/jcs.222463.
Sakata, K., Karaki, H., 1991. Effects of a novel smooth muscle relaxant, KT-362, on contraction and cytosolic Ca2+ level in the rat aorta. Br. J. Pharmacol. 102, 174–178. https://doi.org/10.1111/j.1476-5381.1991.tb12149.x.
Silva, D.F., Araújo, I.G.A., Albuquerque, J.G.F., Porto, D.L., Dias, K.L.G., Cavalcante, K.V. M., Veras, R.C., Nunes, X.P., Barbosa-Filho, J.M., Araújo, D.A.M., Cruz, J.S., Correia, N.A., de Medeiros, I.A., 2011. Rotundifolone-induced relaxation is mediated by BK Ca channel activation and Ca v channel inactivation. Basic Clin. Pharmacol. Toxicol. 109, 465–475. https://doi.org/10.1111/j.1742-7843.2011.00749.x.
Singh, S., Agarwal, K., Iqbal, H., Yadav, P., Yadav, D., Chanda, D., Tandon, S., Khan, F., Gupta, A.K., Gupta, A., 2020. Synthesis and evaluation of substituted 8,8-dimethyl-8H-pyrano[2,3-f]chromen-2-one derivatives as vasorelaxing agents. Bioorg. Med. Chem. Lett 30, 126759. https://doi.org/10.1016/j.bmcl.2019.126759.
Solecki, R.S., 1975. Shanidar IV, a neanderthal flower burial in northern Iraq. Science 80– (190), 880–881. https://doi.org/10.1126/science.190.4217.880.
Tabassum, N., Ahmad, F., 2011. Role of natural herbs in the treatment of hypertension. Pharmacogn.Rev. 5 https://doi.org/10.4103/0973-7847.79097.
Tajada, S., Cidad, P., Colinas, O., Santana, L.F., López-López, J.R., Pérez-García, M.T., 2013. Down-regulation of CaV1.2 channels during hypertension: how fewer CaV1.2 channels allow more Ca2+ into hypertensive arterial smooth muscle. J. Physiol. 591, 6175–6191. https://doi.org/10.1113/jphysiol.2013.265751.
Vasconcelos, J.F., Teixeira, M.M., Barbosa-Filho, J.M., Agra, M.F., Nunes, X.P., Giulietti, A.M., Ribeiro-dos-Santos, R., Soares, M.B.P., 2009. Effects of umbelliferone in a murine model of allergic airway inflammation. Eur. J. Pharmacol. 609, 126–131. https://doi.org/10.1016/j.ejphar.2009.03.027.
Wang, S.P., Zang, W.J., Kong, S.S., Yu, X.J., Sun, L., Zhao, X.F., Wang, S.X., Zheng, X.H., 2008. Vasorelaxant effect of isopropyl 3-(3, 4-dihydroxyphenyl)-2-hydroxypropanoate, a novel metabolite from Salvia miltiorrhiza, on isolated rat mesenteric artery. Eur. J. Pharmacol. 579, 283–288. https://doi.org/10.1016/j.ejphar.2007.10.009.
World Health Organization, et al., 2013. A Global Brief on Hypertension: Silent Killer, Global Public Health Crisis. World Health Day, 2013.
Yang, Y., Li, P.Y., Cheng, J., Mao, L., Wen, J., Tan, X.Q., Liu, Z.F., Zeng, X.R., 2013. Function of BKCa channels is reduced in human vascular smooth muscle cells from han Chinese patients with hypertension. Hypertension 61, 519–525. https://doi.org/10.1161/HYPERTENSIONAHA.111.00211.
Yera, E.R., Cleves, A.E., Jain, A.N., 2011. Chemical structural novelty: on-targets and off-targets. J. Med. Chem. 54, 6771–6785. https://doi.org/10.1021/jm200666a.
Yeturu, K., Chandra, N., 2008. PocketMatch: a new algorithm to compare binding sites in protein structures. BMC Bioinf. 9, 1–17. https://doi.org/10.1186/1471-2105-9-543.
Yu, M., Liu, S.L., Sun, P.B., Pan, H., Tian, C.L., Zhang, L.H., 2016. Peptide toxins and small-molecule blockers of BK channels. Acta Pharmacol. Sin. 37, 56–66. https://doi.org/10.1038/aps.2015.139.
Zhang, Y., Wang, Q.L., Zhan, Y.Z., Duan, H.J., Cao, Y.J., He, L.C., 2010. Role of store-operated calcium entry in imperatorin-induced vasodilatation of rat small mesenteric artery. Eur. J. Pharmacol. 647, 126–131. https://doi.org/10.1016/j.ejphar.2010.08.010.
Zhang, Y., Liao, J., Zhang, L., Li, S., Wu, Y., Shi, L., 2018. BKCa channel activity and vascular contractility alterations with hypertension and aging via β1 subunit promoter methylation in mesenteric arteries. Hypertens. Res. 41, 96–103. https://doi.org/10.1038/hr.2017.96.
Zhou, Y., Xia, X., Lingle, C.J., 2019. The Functionally Relevant Site for Paxilline Inhibition of BK Channels, pp. 1–6. https://doi.org/10.1073/pnas.1912623117.